Organic thermoelectric materials for energy harvesting and temperature control

Boris Russ[1], Anne Glaudell[2]*, Jeffrey J. Urban[1], Michael L. Chabinyc[2] and Rachel A. Segalman[2,3]*

Abstract | Conjugated polymers and related processing techniques have been developed for organic electronic devices ranging from lightweight photovoltaics to flexible displays. These breakthroughs have recently been used to create organic thermoelectric materials, which have potential for wearable heating and cooling devices, and near-room-temperature energy generation. So far, the best thermoelectric materials have been inorganic compounds (such as Bi_2Te_3) that have relatively low Earth abundance and are fabricated through highly complex vacuum processing routes. Molecular materials and hybrid organic–inorganic materials now demonstrate figures of merit approaching those of these inorganic materials, while also exhibiting unique transport behaviours that are suggestive of optimization pathways and device geometries that were not previously possible. In this Review, we discuss recent breakthroughs for organic materials with high thermoelectric figures of merit and indicate how these materials may be incorporated into new module designs that take advantage of their mechanical and thermoelectric properties.

[1]The Molecular Foundry, Lawrence Berkeley National Laboratory, Berkeley, California 94720, USA.
[2]Materials Department, University of California, Santa Barbara, California 93106, USA.
[3]Department of Chemical Engineering, University of California, Santa Barbara, California 93106, USA.
**These authors contributed equally to this work.*

Correspondence to J.J.U., M.L.C. and R.A.S.
jjurban@lbl.gov; mchabinyc@engineering.ucsb.edu; segalman@ucsb.edu

Article number: 16050
doi:10.1038/natrevmats.2016.50
Published online 2 Aug 2016

Semiconducting polymers have recently been demonstrated to exhibit the high electrical conductivity (σ), high Seebeck coefficient (also called thermopower; α or S) and low thermal conductivity (κ) necessary for good thermoelectric performance (the fundamentals of thermoelectrics are summarized in BOX 1). Fully realizing the potential of organic thermoelectrics (OTEs) would deliver flexible energy generation or heating–cooling devices, enabling applications not currently possible with traditional thermoelectrics. OTEs are compatible with inexpensive, scalable processing methods and often possess great mechanical flexibility, which makes them geometrically versatile and lightweight solutions for various applications, such as those requiring an interaction with the human body. Further, the development of these devices will take advantage of molecular design and processing breakthroughs associated with printed organic semiconductors for organic light-emitting diodes (OLEDs)[1,2], organic photovoltaics (OPVs)[3] and organic thin-film transistors (OTFTs)[4].

Significant improvements in the efficiency of traditional inorganic crystalline thermoelectric materials over the past 20 years have been a result of nanostructuring to tune electron and phonon transport[5–7]. These advances have mostly been relevant to high-temperature applications, but for near-ambient applications, the dominant material system is still Bi_2Te_3 and its related alloys[8–10]. Many organic semiconducting materials are stable (unless subjected to photoinduced oxidation) up to 200 °C and are therefore ideally suited for room-temperature applications. Furthermore, because power conversion efficiency scales with the temperature difference divided by the average temperature ($\Delta T/T$), harvesting thermal energy near room temperature using costly modern thermoelectric modules has generally been impractical. Specialized, commercial applications for room-temperature thermoelectrics have instead focused on localized cooling (and heating)[11,12]. To surmount these issues, a substantial effort has been made to identify alternative materials that are scalable both in terms of material availability and manufacturing.

In this Review, we discuss the basic molecular design of organic semiconductors, the critical factors that determine their performance as thermoelectrics and the open questions that must be addressed to control their properties. Several insightful reviews on OTE materials have been published in the past few years[13–19]. We therefore focus primarily on recent developments to highlight the current state of the art, with particular attention on the developing trends in structure–property relationships

Box 1 | **Basic elements of thermoelectrics**

Thermoelectric materials exhibit the Seebeck effect, in which carriers move in response to a temperature gradient. Charge carriers diffuse across the temperature gradient, creating a build up of charge and thus a potential difference, ΔV. The magnitude of this effect is the Seebeck coefficient or 'thermopower', and is simply the potential divided by the applied thermal gradient: $\alpha = -\Delta V/\Delta T$. The thermoelectric performance of a material is generally benchmarked by the dimensionless thermoelectric figure of merit, ZT, which is composed of the electrical conductivity, σ, the thermopower, α (also commonly denoted by S), the thermal conductivity, κ, and the temperature, T:

$$ZT = \frac{\alpha^2\sigma}{\kappa} T$$

A good thermoelectric material has a high ZT, and should be a good electrical conductor (high α) and a poor thermal conductor (low κ). The three thermoelectric parameters σ, α and κ are interrelated with carrier concentration, and decoupling these parameters is decidedly non-trivial. The Seebeck coefficient is directly related to the density of states, whereas the electrical conductivity can be limited by electronic and morphological defects. The Seebeck coefficient reflects the average entropy transported per charge carrier and thus decreases with increasing carrier concentration. By contrast, the electrical conductivity increases with carrier concentration, n, because $\sigma = e\mu n$. The thermal conductivity is composed of a lattice contribution and an electronic contribution, $\kappa = \kappa_L + \kappa_E$; the electronic contribution increases with carrier concentration, as charge carriers can also transport heat.

To accurately assess the thermoelectric performance of a material, σ, α and κ must be evaluated in the same direction as the temperature gradient. This is especially relevant for organic thermoelectric (OTE) materials, because the anisotropy of polymer chains tends to lead to anisotropies in the material after processing, causing the in-plane and out-of-plane properties to differ greatly. In solution-processed thin-film OTE materials, the electrical conductivity and thermopower can be directly measured in the in-plane direction. However, measuring the in-plane thermal conductivity of thin films is difficult. Typically, the thermal conductivity of thin films is measured using the 3ω method (which measures the response to oscillatory heating) or time-domain thermal reflectance, both of which extract the out-of-plane thermal conductivity.

The efficiency, η, of a thermoelectric device (for either power generation or cooling) is related to the ZT of the material and the Carnot limit, $\eta_C = \Delta T/T_H$, which depends on the temperature difference ΔT and the hot-side temperature T_H, through the following equation:

$$\eta = \eta_C \frac{\sqrt{1+ZT}-1}{\sqrt{1+ZT}+1}$$

A prototypical thermoelectric device consists of 'legs' of alternating p- and n-type thermoelectric materials that are connected electrically in series and thermally in parallel, as well as being ZT-matched.

Traditional inorganic thermoelectric devices consist of bulk legs tiled in two dimensions over a ceramic substrate that is patterned with electrical contacts, in which the thermal gradient across the material is perpendicular to the substrate (panel **a**; T_C, cool-side temperature). This geometry is not well suited to many organics and other solution-processed materials, which benefit from an in-plane architecture because the main direction of carrier transport is in the plane of the substrate, as indicated by the current, I, direction. In this geometry (panel **b**), the thermal gradient across the material is parallel to the substrate. This necessitates the development of alternative device geometries to accommodate this processing restriction and also takes advantage of the ability to print OTEs on flexible substrates.

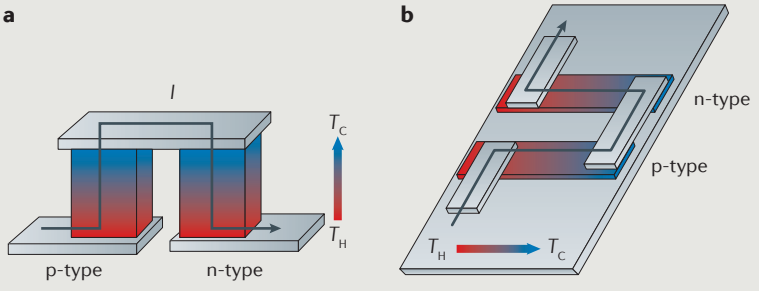

and how these particular properties of flexible thermoelectrics could be used in device and module design. Composite or hybrid thermoelectric materials have been developed to capitalize on the intrinsic strengths of conducting polymers and nanotubes or nanoparticles for thermoelectrics[20–32]. For simple composites, the resulting behaviour is an average of that of both components[33], whereas hybrid materials capitalize on interfacial properties to yield gains in performance exceeding that of the individual components. Although this is an exciting area of development, this Review focuses on single-component materials. As such, composites and hybrids are only briefly discussed.

We identify the basic properties defining thermoelectric performance and highlight the unique materials challenges for OTE materials compared with traditional inorganic thermoelectrics. We then discuss the current state of the art for OTEs, and the progress made in developing and implementing molecular design principles that are relevant to OTEs. We also consider OTE module design and progress towards commercial readiness, and present an outlook on the field of OTEs.

Electronic properties of organic semiconductors

The main difference between the development of new organic materials and of inorganic thermoelectrics is the approach taken to optimize the thermoelectric figure of merit, ZT. A good thermoelectric material is often described as an electronic crystal and a phonon glass[6,33,34]. Inorganic semiconductors are generally the former; thus, focus is placed on reducing the thermal conductivity by increasing phonon scattering to reduce the lattice contribution[34]. By contrast, the thermal conductivity of organic semiconducting materials, particularly polymers, is closer to a phonon glass in many cases. Thus, considerable effort has focused on increasing conduction and maximizing the power factor, $PF = \alpha^2\sigma$, of organic materials.

Organic materials form van der Waals solids with relatively weak electronic coupling between molecules compared with covalent solids; therefore, molecular properties are frequently used as a basis for understanding the solid-state electronic structure[35]. For molecules, these are the highest occupied and lowest unoccupied molecular orbitals (HOMO and LUMO), which form the valence and conduction states in solids[36]. Depending on the molecular design, the gap between these electronic levels typically ranges from ~1 to 3 eV, and the position of the ionization energy and electron affinity with respect to the vacuum level can be shifted as well (FIG. 1). Detailed descriptions of synthetic approaches for effectively modifying energetic levels in organic electronic materials can be found in several excellent reviews[37–40].

Organic semiconductors are relatively insulating as synthesized and, owing to their relatively wide bandgaps, require doping to increase their electrical conductivity. The addition or removal of electrons from the π system of organic molecules causes intramolecular geometric distortions[36]. For this reason, the carriers in organic materials are frequently described as polarons. The polaronic nature of organic materials can be observed using various methods, among which optical spectroscopy is the simplest.

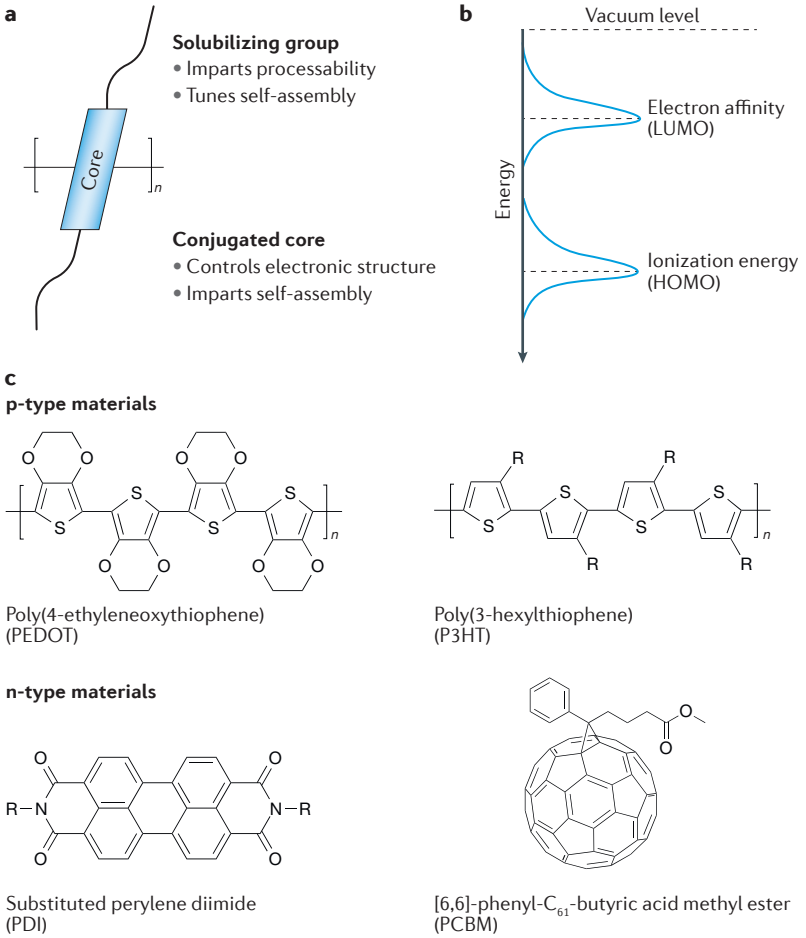

Figure 1 | **Molecular design and energetics of OTE materials. a** | Organic semiconductors and polymers contain conjugated core motifs that enable charge transport. Side chains aid solution processing and can have a role in charge-carrier generation and molecular assembly in the solid state. **b** | The electronic levels of organic materials are given by their ionization energy (approximated by the HOMO) and electron affinity (approximated by the LUMO) that can be tuned by molecular design. Energetic disorder can lead to a distribution of states around these levels for perfectly ordered materials. **c** | Examples of high-performance p- and n-type organic thermoelectric (OTE) molecular structures with favourable molecular ionization energies or electron affinities. States can also be introduced inside the gap through, for example, doping. HOMO, highest occupied molecular orbital; LUMO, lowest unoccupied molecular orbital.

The main optical absorption of the undoped materials undergoes a substantial shift on doping, owing to the formation of polaronic levels; because of geometric relaxation on doping, subgap states are formed, leading to a redshift in the optical absorption[36].

The electrical conductivity of organic materials is affected by both the introduction of carriers and their structural order from the molecular scale to the macroscale[41] (FIG. 2). Within crystalline domains, charge transport can be highly anisotropic, owing to differences in the electronic coupling between molecules[42–44]. The need to couple the π-electronic levels of molecules requires close intermolecular contacts to allow efficient charge transfer between molecules[35]. Conjugation of molecular units leads to planar structures that stack against each other (that is, π stacking) for intermolecular electronic coupling. For example, in semiconducting polymers, the conjugated repeat units are strongly electronically coupled along the backbone and have weaker electronic coupling between stacked chains[43,45]. Functionalities (for example, alkyl chains) added to improve solubility are highly insulating and prevent electronic communication between molecules through the sidechains[46]. Because of these factors, orienting the backbone of polymers along the direction of transport can lead to a significant enhancement of the electrical conductivity relative to non-oriented samples[42]. The ordered domains in organic semiconductors are small (~100 nm) in many cases. The carrier must, therefore, traverse many domains during transport, and as a result, apparent charge mobilities can be markedly lower than might be expected for a perfect single crystal[45]. Because of the structural disorder, along with the polaronic nature of the charge carriers, transport is not well described by band theories used for crystalline inorganic semiconductors, and, in many cases, theories from disordered semiconductors are more successful in rationalizing their behaviour.

Properties of organic thermoelectrics

Reported metrics of OTEs as a function of electrical conductivity are collected in FIG. 3 for a broad range of state-of-the-art doped organic materials; the metrics for the benchmark room-temperature material, Bi_2Te_3, are also shown for comparison. It is clear that the performance of OTE materials operating close to room temperature is rapidly approaching that of their inorganic counterparts. The accelerated pace of improvement of OTEs has been largely enabled by knowledge related to molecular designs and processing conditions that lead to high carrier mobility in OTFTs[4] and high-conductivity electrode layers in OPVs[3]. Because the majority of work conducted on OTEs has focused on optimizing the power factor, we discuss the latest advances for enhancing the electrical conductivity and the Seebeck coefficient in OTEs, and the importance of these studies in terms of future design rules. We also discuss the potential consequences of an enhancement in the power factor on the thermal conductivity, which, for most materials, is strongly dependent on the morphology.

Considering the vast range of available molecular structures of organic materials, it is helpful to consider the performance requirements for potential room-temperature thermoelectrics. Thermoelectric materials must have high electrical conductivities and tunable charge-carrier concentrations. Because the electrical conductivity in the legs of practical thermoelectric modules is more than ~10 S cm^{-1}, it is possible to estimate the requirements for the charge-carrier mobility and carrier concentration, n, in organic materials near room temperature. Considering that the carrier concentration is limited by the molecular density ($n \approx 10^{22}$ cm^{-3} in organic systems), the carrier mobility must be greater than ~0.01 cm^2 V^{-1} s^{-1} to achieve reasonable electrical conductivity at the maximum carrier density. The mobilities of carriers in organic semiconductors, based on field-effect conduction measurements, which are averaged across many domains, are between ~1 and 10 cm^2 V^{-1} s^{-1}, and are comparable to the values reported for doped bulk

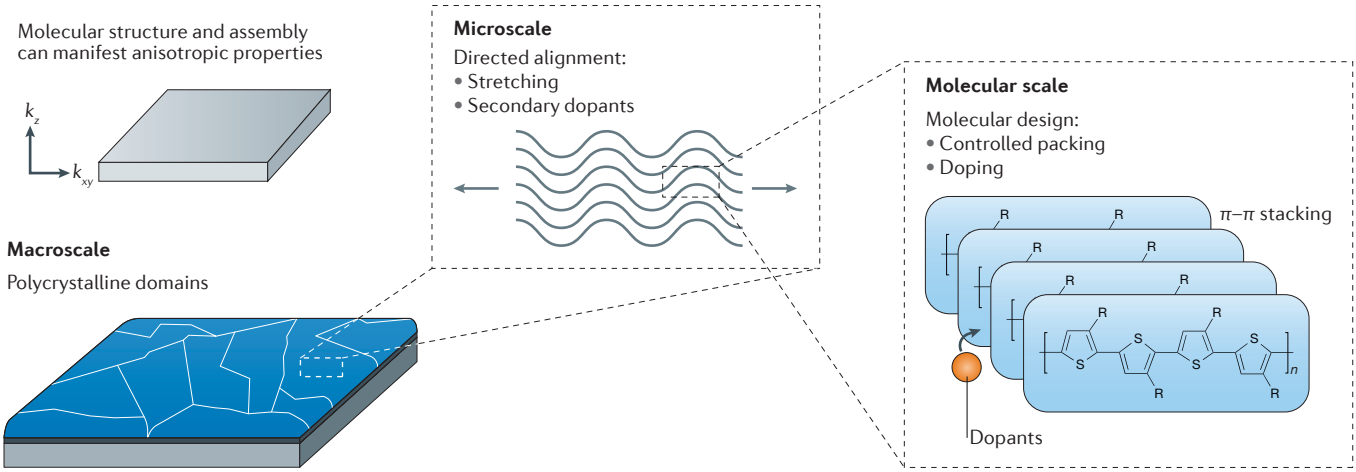

Figure 2 | **Effect of structural order of OTE materials on transport properties.** On the macroscale, polycrystalline domains in solution-deposited organic thermoelectrics (OTEs) can be tens of nanometres to micrometres in size. The orientation of these ordered domains relative to the direction of transport can strongly affect the effective macroscale electrical conductivity. On the microscale, variations in the electronic coupling between molecules and polymeric chains can manifest in highly anisotropic charge transport within individual crystalline domains. Strategies to direct chain alignment, including mechanical stretching and the use of co-solvents, can enhance chain alignment and electronic coupling within domains. On the molecular scale, the conjugation of molecular units leads to planar functionalities that tend to stack against each other, referred to as π–π stacking, for strongest coupling. The molecular design of the planar core motifs, the functionalities (for example, alkyl chains labelled 'R') and the dopant molecules that introduce charge into the assembly provides useful strategies to enhance processability and improve the intermolecular coupling that is necessary for efficient charge transfer between molecules.

materials[4,47–49]. Note that the field-effect mobility, which is measured at a dielectric interface in a thin-film transistor, does not necessarily translate to the bulk mobility in the presence of dopant ions; however, the similarity of the values suggests that it does provide a good guideline. Although metrics such as the mobility help to determine the requirements for electrical conductivity, the dependence of the Seebeck coefficient on carrier concentration is difficult to predict for many materials, making it the largest unknown parameter for organic materials. In the following subsections, we highlight important factors that influence the introduction of carriers into organic semiconductors, how these carriers are transported and their resulting thermopower.

Introducing carriers: doping

Electrical doping of organic materials relies on forming a material that is chemically stable on addition or removal of an electron by a dopant[50]. It is important to understand that, in the literature, the terms p type and n type are frequently used to describe which apparent carrier mobility is largest in a material, rather than the position of the Fermi level. Organic semiconductors can be ambipolar and, in some cases, the hole and electron mobilities are comparable, but one sign of carrier may be preferred owing to the ability to inject or stably dope the material with it[51].

The stability of electrically doped materials is determined, in part, by the ionization energy and electron affinity. The electron affinity of many organic materials is relatively small, which leads to chemical instabilities of negatively charged molecules through reactions with the environment (for example, with water and oxygen)[52,53]. Stable introduction of electron carriers into materials requires the electron affinity to be larger than ~4 eV to avoid reaction with water and oxygen and associated trap states[52–54]. Because of this requirement, stable n-type materials are based on units with relatively large electron affinity, such as perylene diimide (PDI), naphthalene diimide (NDI) and fullerene derivatives[37,55–57]. For the stable introduction of holes, the ionization energy of the semiconductor should be larger than ~5.0 eV for similar reasons.

An example of a widely studied and commercially available, stably doped p-type material is poly(3,4-ethylenedioxythiophene) (PEDOT). PEDOT and its variants are based on the ethylenedioxythiophene (EDOT) monomer because of its simple chemistry and resulting ionization energy of ~5.1 eV. EDOT can be oxidatively polymerized in water in the presence of an acidic polyelectrolyte, typically polystyrenesulfonic acid (PSS), to form a water-processable dispersion, PEDOT:PSS[58]. EDOT can also be polymerized with oxidants from the vapour phase leading to other variants; for example, the oxidant Fe(III) tris-*p*-toluenesulfonate (Tos) can be used to synthesize PEDOT:Tos[59,60]. This simplicity and stability has led to the broad use of EDOT in OTEs.

In an attempt to expand the number of stably doped materials, efforts have focused on the molecular design of dopants, because efficient charge transfer relies on favourable alignment of the frontier electronic levels of the dopant relative to those of the active semiconducting organic material (that is, smaller ionization energies for n-type dopants or larger electron affinities for p-type dopants)[57,61–63]. There are more known p-type dopants than n-type dopants because of the demands

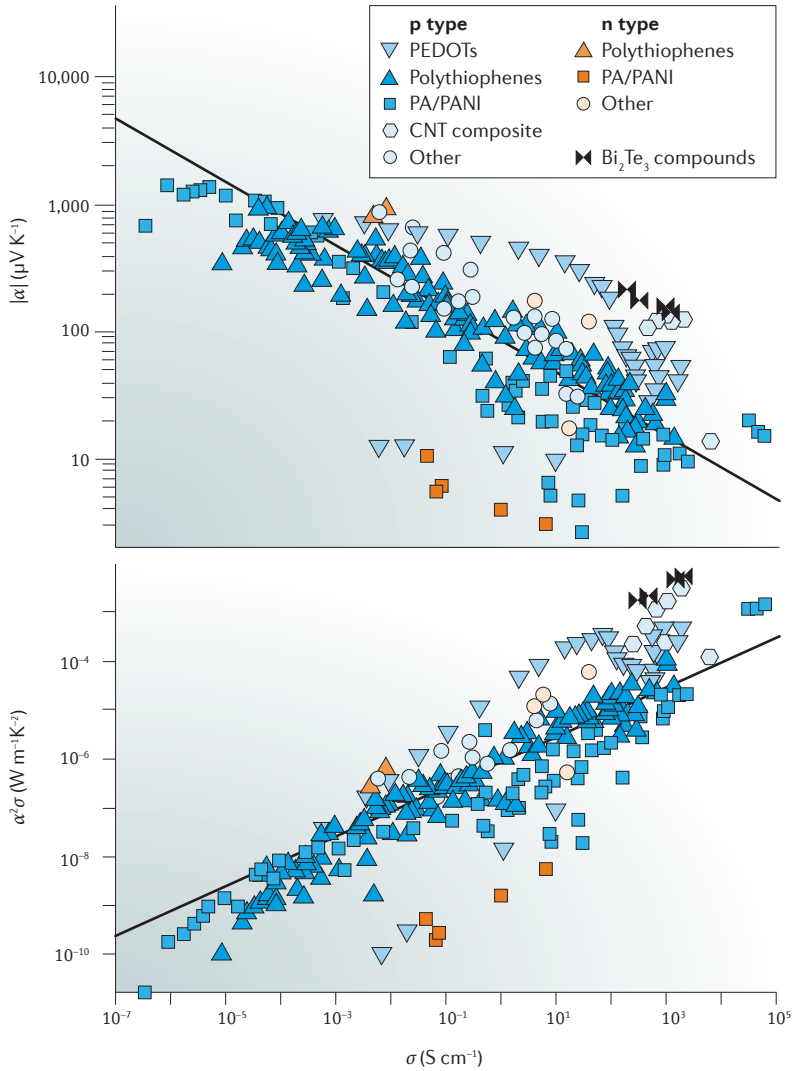

Figure 3 | **The thermoelectric properties of a wide range of OTE materials follow the same empirical trend.** Seebeck coefficient (α; top) and power factor ($\alpha^2\sigma$; bottom) as functions of conductivity (σ) for a range of doped organic thermoelectric (OTE) polymers and composites, are compiled from data reported in the literature. The solid line indicates the empirical relationship $\alpha \propto \sigma^{-1/4}$ (top) and power factor PF $\propto \alpha^{1/2}$ (bottom). The plot includes poly(3,4-ethylenedioxythiophene) (PEDOT)[59,90,95], polythiophenes[80,96,97,106,108,116], polyacetylenes (PA) and polyanilines (PANI)[82,83,109,111], carbon nanotube (CNT) composites[20–22,28,29,157] and other organic molecules[99–102,106]. For reference, the best room-temperature inorganic Bi_2Te_3 compounds are also included[8–10].

for chemical stability of reduced conjugated materials. Although much work has focused on dopants that have clear exothermic charge transfer based on the ionization energy and electron affinity of the polymer and dopant individually[50], recent work has demonstrated good conductivity with dopants for which charge transfer would be expected to be less efficient[64].

New classes of stable dopants for n-type materials have recently emerged. Organometallic dopants have led to impressive performance in both polymers and small molecules[62,65]. Reactive organic dopants have also been developed[66–68]. For example, reagents that lead to hydride transfer, such as 3-(4-dimethylaminobenzylidenyl)-2-indolinone, are efficient dopants for soluble fullerenes and n-type polymers[57,61,69,70]. The addition of trialkylamino-functionalized sidechains to compounds with relatively high electron affinities has also proved to be effective, using a 'latent' approach by the thermally driven transformation of ammonium hydroxide substituents[56,71].

An important design consideration in addition to energetics is the size of the dopant. If a dopant molecule is bulky, it can cause distortions in the intermolecular packing of the semiconductor that may impede charge transport between molecules[50,72–75]. In higher-conductivity materials (above 10 S cm^{-1}), the nominal molar ratio of dopant to conductive units — that is, a monomer in a polymer — can be as large as 1:4 (REF. 72). Even simple dopants, such as I_2, are known to cause substantial changes in the ordered structure of polymers such as poly(3-hexylthiophene) (P3HT)[76]. The incorporation of large amounts of dopant can lead to phase segregation of the doped phase from the undoped phase, which can lower the conductivity[57,70]. In conjugated polyelectrolytes, the counterion to the carrier is covalently attached to the backbone (for example, a sulfonic acid group for a p-type polymer)[77,78]. This structure has generally not led to high electrical conductivity (values are typically <1 S cm^{-1}), but the electrical conductivity in these materials is highly sensitive to simple changes. For example, the change from Na^+ to K^+ as a counterion to the sulfonic acid group can lead to a greater than fivefold decrease in conductivity for a donor–acceptor backbone[78]. The development of structure–property relationships to understand how dopants affect nano- and microstructure in the electrically doped state is an important direction of future research.

Movement of carriers: electrical conductivity

Organic electronic materials are mainly studied as disordered or polycrystalline forms. The mobility of carriers in organic materials is related microscopically to the electronic coupling between molecules and interchain transport in polymers, and macroscopically to the ability of these carriers to cross domain boundaries, similar to polycrystalline inorganic semiconductors. Thus, the observed electrical conductivities of organic materials can vary strongly depending on processing conditions.

Because transport can depend on filling trap states and domain boundaries, the dopant concentration is a major factor in determining the electrical transport properties. For example, nonlinear increases in electrical conductivity with an increasing concentration of dopants are frequently observed when doping semiconducting polymers with molecular dopants, such as tetrafluoro-tetracyanoquinodimethane (F_4TCNQ)[79], or with chemical dopants, such as nitrosonium hexafluorophosphate[80]. Conduction in lightly doped organic materials occurs through thermally assisted processes, with an Arrhenius-type relationship with respect to temperature (that is, conductivity, σ, is proportional to $\exp(-E_A/k_BT)$, where E_A is the activation energy, k_B is the Boltzmann constant and T is the absolute temperature), which is characteristic of charge hopping between nearest neighbours[50,79]. Such temperature dependences can also occur because of barriers at domain boundaries in polycrystalline materials. At high

carrier concentrations, a temperature dependence that suggests variable-range hopping may also emerge, with $\sigma = \sigma_0 \exp[-(T_0/T)^{\gamma}]$, where γ describes the dimensionality of the system ($\gamma = 0.25$ for 3D variable-range hopping and 0.5 for 1D variable-range hopping) and T_0 is the characteristic temperature[42,81–85]. Although these trends can be attributed to filling of the electronic density of states, it is also known that the conductivity can be affected by non-uniformity in materials, which leads to phase-separated domains with high and low conductivity[86]. Most of the work on the microstructure of organic materials has been carried out for undoped materials, making it challenging at this point to separate these two effects.

The processing method influences the electrical conductivity of organic materials as strongly as the carrier concentration. The electrical conductivity of bulk samples of polymers, such as polyacetylene and polythiophene, can be increased by many orders of magnitude by mechanical stretching, leading to alignment of the polymer chains[48]. In solvent-cast materials, processing during coating also affects the resulting conductivity. For example, the addition of co-solvents to a solution of PEDOT:PSS in water can change the electrical conductivity by more than two orders of magnitude without obvious changes in the carrier concentration[87,88]. Another approach taken is simply to remove excess PSS from the blend, thereby reducing the amount of insulator[89,90]. Because of the dependence of the conductivity on such factors, it is difficult to define the upper limits of the conductivity of organic materials, particularly polymers.

The processing method used to introduce dopants to organic semiconductors can have a particularly strong influence on the resulting morphology. For solution-processable materials, a dopant may be added to the casting solution, leading to charge transfer in the solution phase before formation of the solid and changes in solubility[73]. Dopants may also be added after casting by infiltration from the solvent[91–93]. There have not been extensive comparisons of the effects of doping from both methods for the same materials system. Considerable effort has been devoted to studying how F_4TCNQ, a molecule with a relatively deep electron affinity, dopes polymers such as P3HT (REFS 73,91,94). In this materials system, when doped from solution, charge transfer occurs in solution and the resulting conductive film has two phases (heavily doped, and lightly doped or undoped) observed by X-ray diffraction[73]. The charge-transfer reaction in solution limits the solubility of the material, leading to difficulties in directly casting thicker films[91]. The addition of the F_4TCNQ by a sequential spin-coating process can improve the uniformity and result in higher electrical conductivities than those achieved with the traditional blend-and-cast method[91].

Efficient design of thermoelectric modules (as discussed later) requires the integration of both highly conductive p- and n-type materials. Currently, conductivities higher than 100 S cm^{-1} can be readily realized with p-type polymers using various doping methods, and values exceeding 4,000 S cm^{-1} have recently been reported[58,95–98]. These high conductivities were achieved through a combination of improved doping and processing methods. Although there are reports of high-conductivity n-type alkali-doped fullerenes (~550 S cm^{-1})[99–101] and poly(metal 1,1,2,2-ethenetetrathiolate)s (~40 S cm^{-1})[102], typical conductivities are below 1 S cm^{-1} (REFS 56,57,103). Because most effort has been aimed at the study of p-type systems, it is not yet clear whether the lower conductivity of n-type materials is intrinsic or whether this value can be increased with improved materials processing methods and stable dopants.

Entropy of carriers: thermopower

Because of the complex dependence on carrier concentration and microstructure, the thermopower and electrical conductivity in organic materials have different coupling behaviour from those in many inorganic materials. By considering the most basic model of thermopower in homogeneous materials, the electrical conductivity and thermopower are dictated by the density of states (DOS) of the system and the location of the Fermi level, E_F. Only carriers with energy close to the chemical potential (E_F) will participate in transport. The Seebeck coefficient can be defined as the average entropy per charge carrier weighted by the contribution of the carrier to conduction and, thus, directly relates to the conductivity DOS, $\sigma(E)$[104]:

$$\alpha = -\frac{k_B}{e}\int \frac{E - E_F}{k_B T}\,\frac{\sigma(E)}{\sigma}\,dE \qquad (1)$$

Depending on the type of transport present in the system, α can take on various temperature-dependent forms. For lightly doped organic semiconductors, the thermopower is, for the most part, independent of temperature and is consistent with hopping behaviour for a homogeneous system[105]. Such behaviour is not observed in heavily doped polymers, for which the thermopower increases with temperature[106–109]. Our understanding of electronic transport processes is complicated by experimental evidence that clearly does not follow a single transport mechanism, in which the conductivity is thermally activated but the Seebeck coefficient exhibits metallic temperature dependence[110].

Transport models applied to polymers have, for the most part, assumed a homogeneous medium, throughout which carriers are distributed homogeneously with the same transport mechanism[4,48]. The morphology of many doped polymers is poorly understood, but it is known that, in some cases, doping can be inhomogeneous and structural order can vary at the nanoscale. A heterogeneous treatment of electrical conductivity has been previously addressed in light of mixed transport indicated by conductivity and thermopower measurements, with a form similar to how one would treat competing transport mechanisms in a homogeneous, disordered material[111]. The overall resistance ($\rho = 1/\sigma$) of the material is the sum of the contributions of the disordered, σ_d, and ordered, σ_m, regions, with each weighted by a general geometrical factor, f, that reflects the relative amount of each material and the average macroscopic path that a carrier takes through the material:

$$\sigma^{-1} = f_m \sigma_m^{-1} + f_d \sigma_d^{-1} \qquad (2)$$

The behaviour of the Seebeck coefficient is more complex, and it can also be treated using a heterogeneous model[110]. Importantly, the electrical conductivity and Seebeck coefficient can be weighted differently in the ordered and disordered regions owing to the different transport processes in heterogeneous phases. As demonstrated in FIG. 4, mixed transport behaviour may be attributed to varying degrees of heterogeneity and order in the microstructure. The development of models that encompass the heterogeneity of many high-performance polymers should help to improve predictive power in the design of thermoelectric materials.

Direct measurement of the carrier concentration in organic materials is difficult owing to their low mobility and energetic disorder. Hall coefficient measurements have recently been reported for several organic materials, suggesting that, in the future, it may be possible to use such measurements with well-ordered organic semiconductors[85]. Owing to the lack of a predictive model and the difficulty of directly measuring the carrier concentration, it is simplest to discuss observations of thermopower as a function of electrical conductivity. Using literature data for a broad range of doped organic materials (FIG. 3), a striking empirical relationship between the electrical conductivity and thermopower emerges, where $\alpha \propto \sigma^{-1/4}$ ($PF \propto \sigma^{1/2}$)[97,111]. Particularly notable is the fact that these materials exhibit transport mechanisms ranging from hopping to near-metallic conduction. It is unclear why such a relationship occurs because it is not readily predicted from existing transport models. One possibility is that the materials are single-band conductors and their electronic DOS are similar, leading to the observed scaling with electrical conductivity. At this point, this empirical correlation seems to be defied by PEDOT-based systems and polyaniline, suggesting a fertile area for exploration to uncover the origin of the empirical relationship. It is important to note that different approaches and conditions have been used to measure the material thermoelectric properties, most notably the Seebeck coefficient. For example, thermal gradients from ~0.1 to 10 °C have been applied across distances varying from micrometres to centimetres[59,70,90,95,112,113]. These differences can lead to difficulties in the direct comparison of measurements, and the assumptions of the methods should be taken into account for comparative analysis of studies.

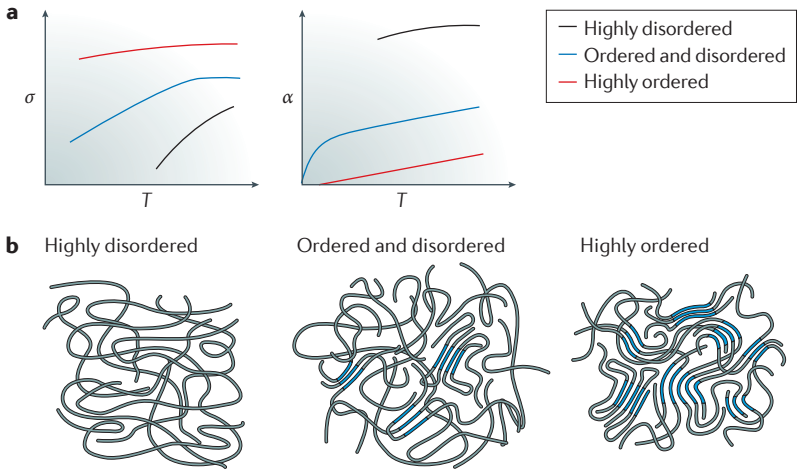

Figure 4 | **Ordered regions connected by disordered chains in semiconducting polymeric materials. a** | Temperature dependences of the electrical conductivity, σ, and the thermopower, α, are shown for organic materials with a spatially homogeneous carrier distribution, but with varying degrees of microstructural/morphological disorder. **b** | The three illustrated material scenarios are: a highly disordered microstructure (left); a highly ordered microstructure (right); and an intermediate microstructure in which both highly ordered and disordered domains exist (centre). Carrier conduction in the highly ordered domain occurs by band conduction with some electronic disorder, whilst carrier conduction in the highly disordered region is assumed to be thermally assisted hopping. From left to right, as the volume fraction of ordered domains increases relative to disordered domains, conductivity increases simply because the average mobility increases. Because of the presence of disordered domains, the overall conductivity may not be metallic-like as a function of temperature even if the ordered regions had metallic bands.

Tuning the degree of doping and morphology is crucial for the optimization of thermoelectric properties in a given system. For example, reported values of the power factor for PEDOT derivatives vary widely owing to changes in processing and the level of doping[59,90,95,112,114]. In PEDOT:Tos, the oxidation level was tuned from 15% to 40% through chemical de-doping, with the maximum power factor of 350 μW m^{-1} K^{-2} achieved at 23% oxidation. The effects of doping on the electronic properties of organic materials are multifaceted. In addition to increasing the charge-carrier concentration, increased doping tends to increase carrier mobility, owing to the filling of trap states caused by energetic disorder. The removal of PSS using an ethylene glycol rinse, for example, was shown to improve all parameters associated with ZT (that is, σ, κ and α), leading to a power factor of 469 μW m^{-1} K^{-2} and a ZT of 0.42, which is the highest ZT reported so far for solution-processable OTEs[90].

Tuning the shape of the electronic DOS is a possible route to enhance the thermopower. For example, narrowing the DOS can help to increase the asymmetry about the Fermi energy and improve the Seebeck coefficient. Relatively high Seebeck coefficients have been reported based on field-effect measurements in highly crystalline small-molecule systems, such as rubrene and pentacene[115], and polymers with relatively small energetic disorder[45]. The DOS can also potentially be tailored in more complex systems. In an effort to simultaneously increase σ and α, an additive, poly(3-hexylthiothiophene) (P3HTT), was added to P3HT to deliberately modify the DOS as a result of different ionization energies of the two polymers[116]. In this case, P3HTT defines the Fermi level, and it is assumed that most of the current is carried in the bulk P3HT. A regime was observed in which both thermopower and conductivity increase with doping modulation using F_4TCNQ; this simultaneous increase was not observed in the neat P3HT system. Although the power factor was quite low compared with that of other systems, this was proof that deliberately introducing DOS asymmetries can help to decouple σ and α.

The polaronic nature of the carriers in organic materials can potentially lead to enhancements in thermopower. The formation of bipolarons from two polarons is considered energetically favourable in homopolymers, such as polythiophene and PEDOT, because this releases structural distortion in the backbone[48]. A significant

enhancement of the Seebeck coefficient (55 μV K^{-1} at an electrical conductivity of ~1,000 S cm^{-1}) in highly ordered vapour-deposited PEDOT:Tos was suggested to occur through the formation of a bipolaron band[95]. The formation of the bipolaron band was inferred from the temperature-dependent transport and photoemission spectra, which were similar to those of a semimetal. Very different behaviour has been observed in other materials, such as polyaniline, which has polaronic carriers and an exceptionally low thermopower (<10 μV K^{-1})[86], at electrical conductivities comparable to those of PEDOT, suggesting that there is still much to be learned about transport in polymers with high carrier densities.

Additionally, strategies that scatter low-energy carriers, whilst allowing high-energy carriers to pass, can increase the asymmetry of mobile carriers above and below the Fermi energy, thereby boosting the Seebeck coefficient[7,33]. The reduction of the total number of charge carriers decreases the electrical conductivity, but because the power factor scales with α^2, a net increase in the power factor can be realized in some regimes of carrier concentration. To identify conditions conducive to these filtering effects, interface engineering efforts have focused on combinations of material components with transport bands that are offset[19,113,117–119]. This phenomenon has been used to explain the properties of some organic–inorganic composite systems[118]; however, a definitive demonstration of energy filtering remains challenging.

Thermal conductivity

Although the thermal conductivity of OTE materials is assumed to be low, it is important to acknowledge the limits of this assumption and its dependence on material properties. The thermal conductivity of amorphous, isotropic undoped organic materials is low, around 0.3 W m^{-1} K^{-1}; however, it is not clear how the thermal conductivity of these disordered materials changes with electrical doping and for different morphologies. It is useful to look at the limits of thermal conductivity in all organic materials to determine the possible ranges of thermal conductivity in OTE materials.

Thermal conductivity, as with any transport property, is a tensor. The most common techniques in use for measuring thermal conductivity (3ω methods (response to oscillatory heating at frequency ω) and time-domain thermoreflectance (TDTR)) are most easily used to measure the out-of-plane conductivity, κ_z. However, because polymeric materials can possess considerable anisotropy, measuring the in-plane conductivity, κ_{xy}, is of paramount importance but remains challenging. Mathematical modelling may be done within 3ω or TDTR measurements of thin films to estimate an anisotropy factor for the thermal conductivity[90,120], the validity of which depends on κ itself. Another option is secondary sample preparation to enable reorientation of the film for compatibility with the TDTR measurement (that is, the in-plane direction becomes the out-of-plane direction). The latter method often requires the ability to make a sufficiently thick film that maintains the order observed in the thin film of interest. This is not necessarily compatible with doping methods, especially post-processing ones.

Fullerenes and fullerene-based molecules have the lowest thermal conductivity of all organic molecules, ranging from 0.03 to 0.1 W m^{-1} K^{-1}. The fullerene C_{60} has a thermal conductivity of ~0.1 W m^{-1} K^{-1}, although this is reduced by the addition of functional groups to make soluble fullerenes; for example, the fullerene derivatives [6,6]-phenyl-C_{61}-butyric acid methyl ester (PCBM) and [6,6]-phenyl-C_{61}-butyric acid *n*-butyl ester (PCBNB) exhibit a 40% lower thermal conductivity[121,122] of 0.06 W m^{-1} K^{-1}. At the higher end of thermal conductivity among organic materials are aligned polymer fibres, in which order is induced mechanically by stretching or pulling the fibres. Insulating liquid crystalline polymer fibres can have axial thermal conductivities as high as 30 W m^{-1} K^{-1}, but also as low as 1 W m^{-1} K^{-1}, illustrating the complexity of estimating anisotropy in κ on the basis of morphology[123]. Inducing order not only reduces phonon scattering, but in electronic polymers may also increase carrier mobility (and thus the electronic contribution to the thermal conductivity, κ_e) by aligning the polymer backbones, reducing traps and increasing connectivity between polymers in the fast-transport direction.

Owing to the difficulty of directly measuring the thermal conductivity of organic thin films in-plane, the reported thermal conductivity (if reported at all) is often the out-of-plane component, κ_z. As shown in fibres and mechanically aligned films, it is clear that anisotropy can significantly affect thermal conductivity in the direction of transport. It is difficult to determine where many classes of the high-performing thermoelectric polymers are positioned on the thermal conductivity spectrum. Many of these materials are locally ordered, some with a degree of long-range order, but have no macroscopic alignment in the *x*–*y* plane without mechanical disturbances. By contrast, polymers are often highly anisotropic out-of-plane, with backbones that are either face-on or edge-on to the substrate, the alignment of which continues through the film in the direction of thickness.

The potential anisotropy of the electronic component to κ_e is also an important consideration, as the high conductivities obtained in PEDOTs and other polymers are measured in the direction of fast transport (that is, in-plane)[124,125]. If carrier transport is extremely anisotropic, κ_{xy} may have a non-negligible electronic component compared with κ_z. In this case, if κ is only measured perpendicular to the direction of carrier transport, it is possible that *ZT* may be misrepresented by an order of magnitude or more.

Anisotropic thermal conductivity has been demonstrated in PEDOT, which is currently the best-performing OTE. The thermal conductivity of PEDOT:PSS is highly anisotropic when using DMSO as a co-solvent, with κ_{xy} as much as double κ_z in undoped films of PEDOT and three times as high as κ_z in treated or doped films[124]. The difference in anisotropy for doped compared with undoped films is attributed to a substantial contribution of charge carriers to κ_e at high electrical conductivity and is described by the Weidemann–Franz law. In another study[126] of PEDOT:PSS with ethylene glycol both as a co-solvent and as a secondary post-processing step, thermal transport was found to be even more anisotropic

($\kappa_{xy} \approx 5.6\kappa_z$). In this case, the anisotropy was attributed to the PSS isolating transport between PEDOT nanocrystals in the out-of-plane direction. In a comparison between DMSO and ethylene glycol co-solvents, DMSO resulted in a lower anisotropy factor ($\kappa_{xy}/\kappa_z = 1.4$ and 1.6, respectively), whereas κ_z was independent of the co-solvent[90]. Using the calculated in-plane conductivity, a record ZT for organic materials was reported with DMSO as the co-solvent ($ZT = 0.42$); a ZT of 0.28 was found for ethylene glycol. Although there was no speculation on the reason for the difference in thermal anisotropy between using DMSO and ethylene glycol co-solvents, this illustrates that rational control of thermal asymmetry is a promising route to enhance ZT.

System design

Thermoelectric module design using inorganic thermoelectric materials is well-established, with commercial devices on the market for both power generation and solid-state cooling and heating applications[12]. Development of OTE modules is currently at a proof-of-principle stage and makes use of developments in printing methods for OTFTs, OLEDs and OPVs for both large-area and wearable applications[1–4,127–129] (FIG. 5a). The flexible and lightweight nature of OTEs offers the potential for low-temperature applications that are impractical for rigid inorganics, such as personal temperature control using OTE coolers (OTEC) and wearable energy harvesting using OTE generators (OTEG). Such OTE systems would offer dual-modality operation (for example, either for cooling or power generation), whereby the functionality could, in principle, be switched back and forth on demand. Although many challenges remain, OTEs offer promise to effectively address the requirements of thermal-management materials, such as flexibility, tailored device architecture, low-energy processing and personal comfort (for example, lightweight and breathable materials). In this section, we highlight the potential of OTE devices and discuss recent progress towards their realization.

Wearable and biointegrated devices have attracted considerable attention[127–129]; however, suitable power sources remain to be developed. An integrated power source that makes use of body heat has the potential to provide continuous power without downtime for battery charging or replacement. In applications such as artificial skins, point-of-care diagnostics, biological actuators and short-range communication, devices require micro- to milliwatts of power, and body heat can enable sufficient energy harvesting for operation[128,129]. To illustrate this energy-harvesting potential, we can consider the human body as a heat engine that releases about 100 W of thermal energy under basal metabolic conditions (operating near 37 °C)[130]. The operation of a state-of-the-art TEG (assuming $ZT \approx 1$) under optimal harvesting conditions with an ambient temperature of 20 °C would generate electricity with ~0.6% efficiency (owing to Carnot limitations). Therefore, it is possible to harvest an appreciable power density of ~30 μW cm^{-2} for OTE applications (~600 mW of the total power from the entire body, assuming a body surface area of ~1.5 m^2. Flexible OTEs can uniquely enable the conformal contact with the body that is necessary to ensure efficient heat transfer to realize these projected power densities.

Architecture of modules

Conversion efficiencies in thermoelectric devices are limited by parasitic losses due to thermal conduction through the materials (that is, heat leaking from the hot side to the cold side of the thermoelectric legs, as illustrated in BOX 1) and to Joule heating (proportional to I^2R) generated by the induced thermoelectric current, I, flowing through legs of resistance R. Although single-carrier-type (n- or p-) leg devices can be constructed, connecting alternating n- and p-type legs electrically in series (and thermally in parallel) enables more efficient interconnects, decreasing parasitic thermal leakages and allowing maximum power generation from a heat source. Having many legs in series allows one to establish large voltages across the device, which are necessary to meet minimum thresholds for device operation. Representative power densities (μW cm^{-2}) and thermoelectric material properties of the highest performing p-type and n-type OTEs are shown in FIG. 5d.

Module performance is dependent not only on the thermoelectric material properties of the elements, but also on the leg geometries and leg spacing within the device, as illustrated in FIG. 5d–f. For example, increasing the leg length or decreasing the leg cross-section allows larger ΔT across the thermoelectric generator but increases the Joule heating losses. In addition to leg geometry, the fill factor (the amount of space in a module taken up by thermoelectric elements) must also be considered for performance optimization (FIG. 5e). A smaller fill factor reduces the total number of thermoelectric elements that make up the module, which allows a higher sustainable ΔT across the thermoelectric generator (increasing the potential for energy harvesting) but, at the same time, limits the contribution of the elements in parallel to power generation. Higher fill factors generally result in larger power outputs for OTE materials.

To maximize conversion of heat into electricity, both electrical and thermal matching conditions must be satisfied (FIG. 5c). The internal module resistance must be matched to the external electrical load resistance ($R = R_L$). Concurrently, the thermal resistances of the thermoelectric and the heat exchangers or heat spreaders connected to it must also be matched ($\theta_{TE} = \theta_{heat\ rejection}$)[11]. We note that a consequence of this thermal matching condition is that under maximum power generation, ΔT across the thermoelectric generator is only half the temperature difference between the source and ambient temperatures, ($T_H - T_C$) = 0.5($T_H - T_{ambient}$). For some applications, natural convection may be sufficient for heat rejection, which can help to reduce device complexity and cost[131]. Further details on thermal and electrical matching considerations in module design can be found in several excellent articles[11,12,132,133].

To maintain sufficient temperature gradients for effective thermoelectric operation, the heat transfer direction in OTE legs must be millimetres to centimetres in thickness[11,134,131]. Because low-cost processing

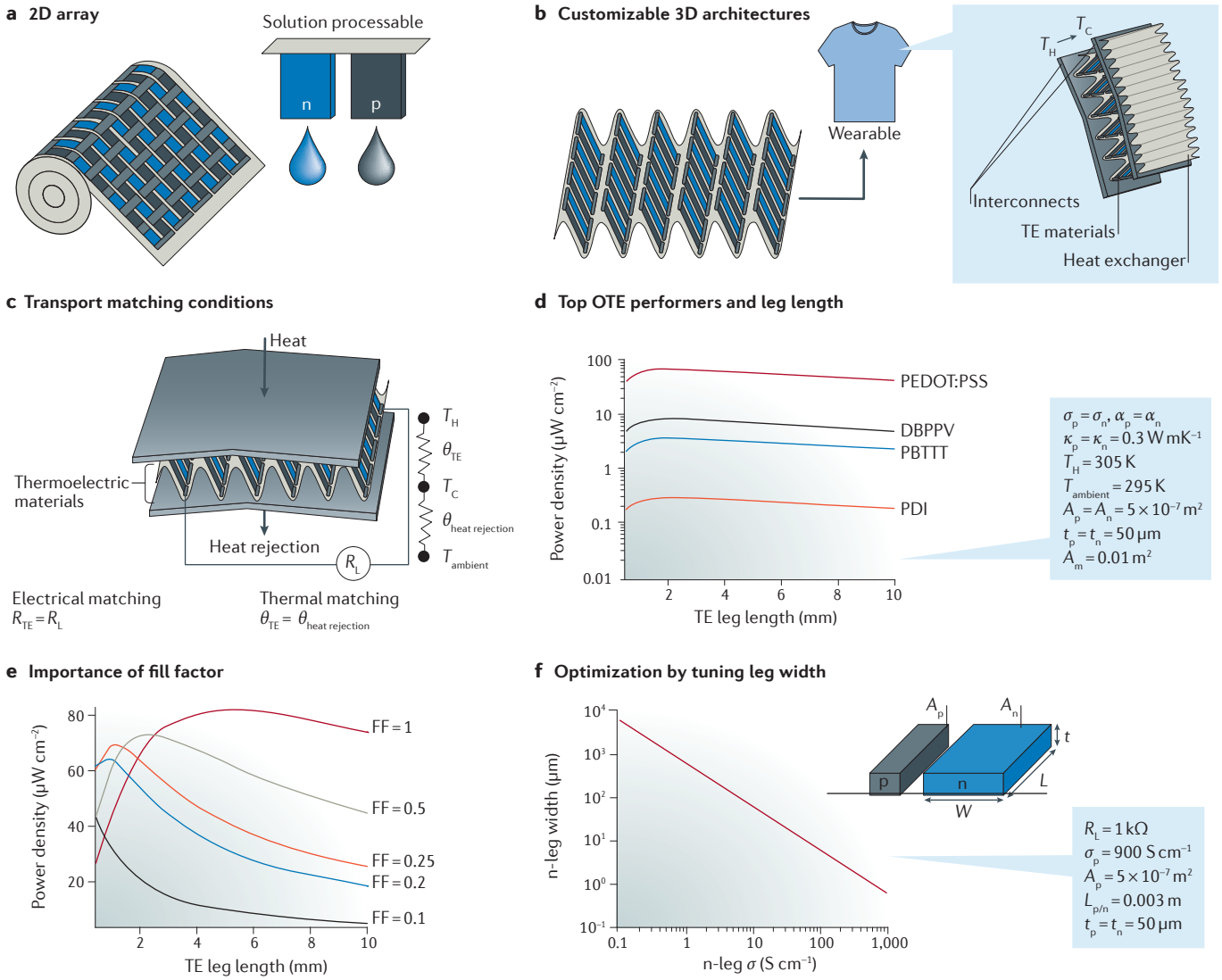

Figure 5 | **OTE materials compatible with high-throughput 2D processing enable customizable and easily optimizable device architectures. a** | Solution-processable p-type and n-type organic thermoelectric (OTE) materials can be printed in a roll-to-roll process. **b** | 2D arrays are transformable into flexible and lightweight 3D structures ideal for wearable applications. **c** | Optimization of OTE performance requires the consideration of both thermal and electrical transport trade-offs. **d** | The length (*L*) of the p-type and n-type legs affects the power density of thermoelectric devices; the representative range of power densities using thermoelectric performance metrics for the highest performing p-type (PEDOT:PSS[90] and PBTTT[97]) and n-type (DBPPV[70] and PDI[56]) materials are shown. **e** | The fill factor (FF) also has a pronounced effect on the achievable power densities of the device, illustrated using performance metrics of PEDOT:PSS[90]. **f** | Printing techniques enable versatility in tuning widths (*W*), and thereby cross-sections ($A_{p/n}$), of OTE legs to match the electrical resistance for a given pair of p–n materials (R_{TE}) with the external-load electrical resistance (R_L) for optimal device performance. Here, representative widths of the n leg needed to match a fixed 1-kΩ external load are shown as functions of the electrical conductivity of the n-leg component. θ, thermal resistance; A_m, module cross-sectional area; DBPPV, 2,3-dibutoxy-1,4-poly(phenylenevinylene); PBTTT, poly(2,5-bis(3-alkylthiophen-2-yl) thieno[3,2-*b*]thiophene); PDI, perylene diimide; PEDOT, poly(3,4-ethylenedioxythiophene); PSS, polystyrenesulfonic acid; T_C, cool-side temperature; T_H, hot-side temperature; $t_{p,n}$, leg thickness; TE, thermoelectric.

approaches (for example, roll-to-roll, gravure and ink-jet) typically deposit nano- to micrometre-thick thin films on a substrate, designs for heat transfer in the in-plane direction of these elements is most appropriate for module architectures. Creative strategies, such as origami, rolled or corrugated[131,135] designs inspired by battery technologies, can be used to convert 2D printed arrays of thin-film legs into 3D architectures with the thermal gradient running parallel to the substrate, as illustrated in FIG. 5a,b. Generating such 3D architectures ensures compatibility with large-area heat sources[32,131]. Because printing techniques allow the simple adjustment of leg widths in the deposited arrays, cross-sectional areas of n or p legs can be easily controlled to optimize device performance for specific combinations of materials (FIG. 5f).

Prototype organic thermoelectric generators

Flexible thermoelectric devices have been demonstrated by both academic and industrial research groups using organic materials either as sacrificial binders of active inorganic materials (that are subsequently burned out at high temperatures)[136–138], or as active materials in their own right, or as part of composite or hybrid systems[139]. In this subsection, we focus the discussion on device developments using single-component OTE materials, in which the design route fully utilizes the deposited material and is compatible with low-temperature processing.

Organometallic polymers have demonstrated the highest OTEG performance so far, with an attained power output of ~1 μW cm^{-2} under a 30-K temperature differential[102]. These polymers are poorly processable and require pressed pellets and the use of traditional thermoelectric cross-plane geometries. Using high-performance, solution-processable OTE materials, TEGs with power outputs of up to hundreds of nW cm^{-2} with carbon nanotube[32,77,140,141] and PEDOT-based systems[59,139,142] have been demonstrated. For industrial and practical implementation of OTE materials, researchers have focused on design strategies for solution-processable materials that are compatible with modern lithographic techniques and roll-to-roll processing. In a hybrid approach using photolithography and solution-processable methods[59], an OTEG prototype using 30-μm-thick PEDOT:Tos p-type and TTF–TCNQ n-type legs produced an output power of 5–25 nW cm^2 at ~5–10 °C. Large-area roll-to-roll printing has been used to fabricate a proof-of-principle TEG with PEDOT:PSS assembled into 18,000 junctions, each being 1.2-μm thick with silver interconnects on polyethylene terephthalate foil[142]. The rolled-up device did not exceed picowatt-level total power generation; however, this demonstration did emphasize the high-throughput potential for thermoelectric module development. A parallel series of legs is one strategy for ensuring that the device continues working even when one element fails[142]. In another interesting example highlighting the consideration of breathability in fabrics, PEDOT:PSS was coated on polyester textile fibres to form a TEG resulting in the harvesting of nanowatt-level total power[139].

Outlook and conclusions

Organic materials offer opportunities to construct thermoelectric modules with different designs from those made from traditional inorganic materials. Accompanying the new opportunities that OTEs offer, however, are challenges both in gaining a fundamental understanding of thermoelectric behaviour in organic conductors and also in translating this behaviour into better-performing modules. We highlight below several emerging areas for further material development as examples of the possible horizons in the field of OTEs.

The development of open-shell, stable radical polymers and molecules provides a set of materials with electronic structures that are substantially different from existing organic semiconductors[143,144]. For example, pendant stable radicals can be attached to insulating main chains for hopping conduction upon partial oxidation or reduction. Recent efforts have shown that the addition of stable radicals to PEDOT can provide a pathway for boosting the Seebeck coefficient without influencing the electrical conductivity[144].

Looking beyond improving traditional electron and hole transport in conjugated frameworks, another possible means of enhancing the thermoelectric transport is to incorporate the relatively high ionic conductivity (as high as 1 S cm^{-1}) of some polymers. These high ionic conductivities can be obtained together with electronic conduction, leading to organic mixed ion–electron conductors[145]. It has recently been suggested that this ability to simultaneously carry appreciable electronic and ionic charge can lead to unique thermoelectric properties[146], but the way that these transport properties influence each other within a single material is poorly understood. Recent publications suggest that combining electrochemical reactions with thermoelectric behaviour in organic materials can lead to improved performance[147,148].

Further, the flexibility in the design of such devices opens the possibility for improving performance and efficiencies beyond those of traditional designs by using unconventional geometrical architectures. One example is the use of cascading thermoelectric elements, which are easier to realize with solution-processed polymers that have no lattice-matching constraints. These devices could benefit from innovative heat-engine cycles, such as the Ericsson cycle, and maximize the use of heat gradients by using spiral or braided counter-current exchange geometries not available to rigid materials[149,150]. Creating graded materials offers the potential for expanding energy-conversion efficiencies in these devices by matching the thermal gradients to a gradient in the Seebeck coefficient[151]. OTECs may offer possibilities for supercooling phenomena[152], which are challenging to realize in conventional systems. Architectural design may also benefit from harnessing molecular design and processing to tailor material anisotropies in preferred transport directions. The thermoelectric behaviour and flexibility of OTE materials could enable applications beyond OTEG and OTECs, such as dual-parameter sensors[1,153]. Ultimately, transitioning from 'efficiency-driven' to 'deployment-driven' material designs may prove helpful in expanding the utility of thermoelectric technology, as has been the case for other fields of power generation. New deployment-relevant metrics for thermoelectric materials, such as the price per unit power, that can help to weigh the economic impact of fabrication, manufacturing and system engineering are currently being developed[11,117,134,154,155].

Although OTE materials have now been demonstrated to have figures of merit within the range of inorganic materials, our understanding of how the unique transport physics of organic materials affects the thermoelectric performance is in its infancy. For this reason, the true limits of the potential for OTEs are not yet known. Further, completely new materials designs have great opportunity to disrupt the pathway towards OTE modules. An understanding of the limits of the power

factor as well as the thermal conductivity in these anisotropic materials, will motivate module designs that take advantage of both solution-processing routes and the fact that the specific combination of σ, α and κ will be very different from those of the inorganic materials for which thermoelectric module design was first envisaged. The realization of thermal management offers opportunities for personal comfort applications and thus broader energy mitigation: for example, reducing the large energy consumption of heating and cooling commercial and residential buildings. Interestingly, the sensitivity of skin receptors to small changes in heat flux means that the perception of 'thermal comfort' does not truly correspond to absolute temperature conditions, and a sensation of cooling can be realized with a relatively small temperature change (<1 °C)[156]. Therefore, with creative approaches to managing heat flux and designing robust conformal contacts with the skin for heat transfer, it may be possible to achieve efficient localized cooling and heating devices. We hope that in this Review we have conveyed the exciting opportunities for fundamental insight in materials design, processing strategies, module architectures and the eventual application of OTEs.

1. Lee, J. *et al.* Deep blue phosphorescent organic light-emitting diodes with very high brightness and efficiency. *Nat. Mater.* **15**, 92–98 (2016).
2. Reineke, S., Thomschke, M., Lüssem, B. & Leo, K. White organic light-emitting diodes: status and perspective. *Rev. Mod. Phys.* **85**, 1245–1293 (2013).
3. Dou, L. *et al.* 25th anniversary article. A decade of organic/polymeric photovoltaic research. *Adv. Mater.* **25**, 6642–6671 (2013).
4. Sirringhaus, H. 25th anniversary article. Organic field-effect transistors: the path beyond amorphous silicon. *Adv. Mater.* **26**, 1319–1335 (2014).
5. Cahill, D. G. *et al.* Nanoscale thermal transport. *J. Appl. Phys.* **93**, 793–818 (2003).
6. Snyder, G. J. & Toberer, E. S. Complex thermoelectric materials. *Nat. Mater.* **7**, 105–114 (2008).
7. Vineis, C. J., Shakouri, A., Majumdar, A. & Kanatzidis, M. G. Nanostructured thermoelectrics: big efficiency gains from small features. *Adv. Mater.* **22**, 3970–3980 (2010).
8. Goldsmid, H. J. The electrical conductivity and thermoelectric power of bismuth telluride. *Proc. Phys. Soc. Lond.* **71**, 633–646 (1958).
9. Poudel, B. *et al.* High-thermoelectric performance of nanostructured bismuth antimony telluride bulk alloys. *Science* **320**, 634–638 (2008).
10. Venkatasubramanian, R., Siivola, E., Colpitts, T. & O'Quinn, B. Thin-film thermoelectric devices with high room-temperature figures of merit. *Nature* **413**, 597–602 (2001).
11. Priya, S. & Inman, D. J. *Energy Harvesting Technologies* Vol. 21 (Springer, 2009).
12. Rowe, D. M. *Thermoelectrics Handbook: Macro to Nano* (CRC, 2005).
13. Bubnova, O. & Crispin, X. Towards polymer-based organic thermoelectric generators. *Energy Environ. Sci.* **5**, 9345–9362 (2012).
14. Chen, Y., Zhao, Y. & Liang, Z. Solution processed organic thermoelectrics: towards flexible thermoelectric modules. *Energy Environ. Sci.* **8**, 401–422 (2015).
15. Poehler, T. O. & Katz, H. E. Prospects for polymer-based thermoelectrics: state of the art and theoretical analysis. *Energy Environ. Sci.* **5**, 8110–8115 (2012).
16. Yang, J. H., Yip, H. L. & Jen, A. K. Y. Rational design of advanced thermoelectric materials. *Adv. Energy Mater.* **3**, 549–565 (2013).
17. Zhang, Q., Sun, Y., Xu, W. & Zhu, D. Organic thermoelectric materials: emerging green energy materials converting heat to electricity directly and efficiently. *Adv. Mater.* **26**, 6829–6851 (2014).
18. Chabinyc, M. L., Schiltz, R. A. & Glaudell, A. M. in *Innovative Thermoelectric Materials* (eds Katz, H. E. & Poehler, T. O.) (Imperial College Press, 2016).
19. Urban, J. J. & Coates, N. E. in *Innovative Thermoelectric Materials* (eds Katz, H. E. & Poehler, T. O.) (Imperial College Press, 2016).
20. Moriarty, G. P., Briggs, K., Stevens, B., Yu, C. & Grunlan, J. C. Fully organic nanocomposites with high thermoelectric power factors by using a dual-stabilizer preparation. *Energy Technol.* **1**, 265–272 (2013).
21. Kim, D., Kim, Y., Choi, K., Grunlan, J. C. & Yu, C. H. Improved thermoelectric behavior of nanotube-filled polymer composites with poly(3,4-ethylenedioxythiophene poly(styrenesulfonate). *ACS Nano* **4**, 513–523 (2010).
22. Choi, K. & Yu, C. Highly doped carbon nanotubes with gold nanoparticles and their influence on electrical conductivity and thermopower of nanocomposites. *PloS One* **7**, e44977 (2012).
23. Coates, N. E. *et al.* Effect of interfacial properties on polymer-nanocrystal thermoelectric transport. *Adv. Mater.* **25**, 1629–1633 (2013).
24. Yee, S. K., Coates, N. E., Majumdar, A., Urban, J. J. & Segalman, R. A. Thermoelectric power factor optimization in PEDOT:PSS tellurium nanowire hybrid composites. *Phys. Chem. Chem. Phys.* **15**, 4024–4032 (2013).
25. Ireland, R. M. *et al.* Effects of pulsing and interfacial potentials on tellurium–organic heterostructured films. *ACS Appl. Mater. Interface* **5**, 1604–1611 (2013).
26. Ireland, R. M., Zhang, L. S., Gopalan, P. & Katz, H. E. Tellurium thin films in hybrid organic electronics: morphology and mobility. *Adv. Mater.* **25**, 4358–4364 (2013).
27. Sinha, J., Ireland, R. M., Lee, S. J. & Katz, H. E. Synergistic thermoelectric power factor increase in films incorporating tellurium and thiophene-based semiconductors. *MRS Commun.* **3**, 97–100 (2013).
28. Yu, C., Choi, K., Yin, L. & Grunlan, J. C. Light-weight flexible carbon nanotube based organic composites with large thermoelectric power factors. *ACS Nano* **5**, 7885–7892 (2011).
29. Yu, C., Kim, Y. S., Kim, D. & Grunlan, J. C. Thermoelectric behavior of segregated-network polymer nanocomposites. *Nano Lett.* **8**, 4428–4432 (2008).
30. Hardigree, J. F. M. *et al.* Reducing leakage currents in n-channel organic field-effect transistors using molecular dipole mono layers on nanoscale oxides. *ACS Appl. Mater. Interfaces* **5**, 7025–7032 (2013).
31. Dun, C. *et al.* Layered Bi_2Se_3 nanoplate/polyvinylidene fluoride composite based n-type thermoelectric fabrics. *ACS Appl. Mater. Interfaces* **7**, 7054–7059 (2015).
32. Hewitt, C. A. *et al.* Multilayered carbon nanotube/polymer composite based thermoelectric fabrics. *Nano Lett.* **12**, 1307–1310 (2012).
33. Shakouri, A. Recent developments in semiconductor thermoelectric physics and materials. *Annu. Rev. Mater. Res.* **41**, 399–431 (2011).
34. Beekman, M., Morelli, D. T. & Nolas, G. S. Better thermoelectrics through glass-like crystals. *Nat. Mater.* **14**, 1182–1185 (2015).
35. Coropceanu, V. *et al.* Charge transport in organic semiconductors. *Chem. Rev.* **107**, 926–952 (2007).
36. Bredas, J. L. & Street, G. B. Polarons, bipolarons, and solitons in conducting polymers. *Acc. Chem. Res.* **18**, 309–315 (1985).
37. Anthony, J. E., Facchetti, A., Heeney, M., Marder, S. R. & Zhan, X. n-Type organic semiconductors in organic electronics. *Adv. Mater.* **22**, 3876–3892 (2010).
38. Guo, X., Baumgarten, M. & Müllen, K. Designing π-conjugated polymers for organic electronics. *Prog. Polym. Sci.* **38**, 1832–1908 (2013).
39. Holliday, S., Donaghey, J. E. & McCulloch, I. Advances in charge carrier mobilities of semiconducting polymers used in organic transistors. *Chem. Mater.* **26**, 647–663 (2014).
40. Mei, J. & Bao, Z. Side chain engineering in solution-processable conjugated polymers. *Chem. Mater.* **26**, 604–615 (2014).
41. Chabinyc, M. Thermoelectric polymers: behind organics' thermopower. *Nat. Mater.* **13**, 119–121 (2014).
42. Heeger, A. J., Kivelson, S., Schrieffer, J. & Su, W.-P. Solitons in conducting polymers. *Rev. Mod. Phys.* **60**, 781 (1988).
43. Noriega, R. *et al.* A general relationship between disorder, aggregation and charge transport in conjugated polymers. *Nat. Mater.* **12**, 1038–1044 (2013).
44. Rivnay, J. *et al.* Large modulation of carrier transport by grain-boundary molecular packing and microstructure in organic thin films. *Nat. Mater.* **8**, 952–958 (2009).
45. Venkateshvaran, D. *et al.* Approaching disorder-free transport in high-mobility conjugated polymers. *Nature* **515**, 384–388 (2014).
46. Mei, J. G., Kim, D. H., Ayzner, A. L., Toney, M. F. & Bao, Z. A. Siloxane-terminated solubilizing side chains: bringing conjugated polymer backbones closer and boosting hole mobilities in thin-film transistors. *J. Am. Chem. Soc.* **133**, 20130–20133 (2011).
47. Fabretto, M. V. *et al.* Polymeric material with metal-like conductivity for next generation organic electronic devices. *Chem. Mater.* **24**, 3998–4003 (2012).
48. Heeger, A. J. Semiconducting and metallic polymers: the fourth generation of polymeric materials†. *J. Phys. Chem. B* **105**, 8475–8491 (2001).
49. Worfolk, B. J. *et al.* Ultrahigh electrical conductivity in solution-sheared polymeric transparent films. *Proc. Natl Acad. Sci. USA* **112**, 14138–14143 (2015).
50. Walzer, K., Maennig, B., Pfeiffer, M. & Leo, K. Highly efficient organic devices based on electrically doped transport layers. *Chem. Rev.* **107**, 1233–1271 (2007).
51. Zaumseil, J. & Sirringhaus, H. Electron and ambipolar transport in organic field-effect transistors. *Chem. Rev.* **107**, 1296–1323 (2007).
52. Anthopoulos, T. D., Anyfantis, G. C., Papavassiliou, G. C. & de Leeuw, D. M. Air-stable ambipolar organic transistors. *Appl. Phys. Lett.* **90,** 122105 (2007).
53. de Leeuw, D. M., Simenon, M. M. J., Brown, A. R. & Einerhand, R. E. F. Stability of n-type doped conducting polymers and consequences for polymeric microelectronic devices. *Synth. Met.* **87**, 53–59 (1997).
54. Nicolai, H. T. *et al.* Unification of trap-limited electron transport in semiconducting polymers. *Nat. Mater.* **11**, 882–887 (2012).
55. Jung, B. J., Tremblay, N. J., Yeh, M.-L. & Katz, H. E. Molecular design and synthetic approaches to electron-transporting organic transistor semiconductors†. *Chem. Mater.* **23**, 568–582 (2011).
56. Russ, B. *et al.* Power factor enhancement in solution-processed organic n-type thermoelectrics through molecular design. *Adv. Mater.* **26**, 3473–3477 (2014).
57. Schlitz, R. A. *et al.* Solubility-limited extrinsic n-type doping of a high electron mobility polymer for thermoelectric applications. *Adv. Mater.* **26**, 2825–2830 (2014).
58. Shi, H., Liu, C., Jiang, Q. & Xu, J. Effective approaches to improve the electrical conductivity of PEDOT:PSS: a review. *Adv. Electron. Mater.* **1**, 1500017 (2015).
59. Bubnova, O. *et al.* Optimization of the thermoelectric figure of merit in the conducting polymer poly(3,4-ethylenedioxythiophene). *Nat. Mater.* **10**, 429–433 (2011).
This paper demonstrated routes for tuning the thermoelectric properties of PEDOT for optimal performance and demonstrated a first proof-of-principle OTE device.
60. Winther-Jensen, B. & West, K. Vapor-phase polymerization of 3,4-ethylenedioxythiophene: a route to highly conducting polymer surface layers. *Macromolecules* **37**, 4538–4543 (2004).
61. Wei, P. *et al.* 2-(2-Methoxyphenyl)-1,3-dimethyl-1H-benzoimidazol-3-ium iodide as a new air-stable n-type dopant for vacuum-processed organic semiconductor thin films. *J. Am. Chem. Soc.* **134**, 3999–4002 (2012).
62. Guo, S. *et al.* n-Doping of organic electronic materials using air-stable organometallics. *Adv. Mater.* **24**, 699–703 (2012).

63. Lussem, B., Riede, M. & Leo, K. Doping of organic semiconductors. *Phys. Status Solidi A* **210**, 9–43 (2013).
64. Li, J. *et al.* Introducing solubility control for improved organic p-type dopants. *Chem. Mater.* **27**, 5765–5774 (2015).
65. Qi, Y. *et al.* Solution doping of organic semiconductors using air-stable n-dopants. *Appl. Phys. Lett.* **100**, 083305 (2012).
66. Chan, C. K., Kim, E. G., Brēdas, J. L. & Kahn, A. Molecular n-type doping of 1,4,5,8-naphthalene tetracarboxylic dianhydride by pyronin B studied using direct and inverse photoelectron spectroscopies. *Adv. Funct. Mater.* **16**, 831–837 (2006).
67. Li, F. *et al.* Acridine orange base as a dopant for n doping of C_{60} thin films. *J. Appl. Phys.* **100**, 23716–23900 (2006).
68. Li, F., Werner, A., Pfeiffer, M., Leo, K. & Liu, X. Leuco crystal violet as a dopant for n-doping of organic thin films of fullerene C_{60}. *J. Phys. Chem. B* **108**, 17076–17082 (2004).
69. Naab, B. D. *et al.* Mechanistic study on the solution-phase n-doping of 1,3-dimethyl-2-aryl-2,3-dihydro-1H-benzoimidazole derivatives. *J. Am. Chem. Soc.* **135**, 15018–15025 (2013).
70. Shi, K. *et al.* Toward high performance n-type thermoelectric materials by rational modification of BDPPV backbones. *J. Am. Chem. Soc.* **137**, 6979–6982 (2015).
71. Russ, B. *et al.* Tethered tertiary amines as solid-state n-type dopants for solution-processable organic semiconductors. *Chem. Sci.* **7**, 1914–1919 (2016).
72. Cochran, J. E. *et al.* Molecular interactions and ordering in electrically doped polymers: blends of PBTTT and F_4TCNQ. *Macromolecules* **47**, 6836–6846 (2014).
73. Duong, D. T., Wang, C., Antono, E., Toney, M. F. & Salleo, A. The chemical and structural origin of efficient p-type doping in P3HT. *Org. Electron.* **14**, 1330–1336 (2013).
74. Winokur, M. *et al.* X-ray scattering from sodium-doped polyacetylene: incommensurate–commensurate and order–disorder transformations. *Phys. Rev. Lett.* **58**, 2329 (1987).
75. Winokur, M., Wamsley, P., Moulton, J., Smith, P. & Heeger, A. Structural evolution in iodine-doped poly (3-alkylthiophenes). *Macromolecules* **24**, 3812–3815 (1991).
76. Tashiro, K., Kobayashi, M., Kawai, T. & Yoshino, K. Crystal structural change in poly(3-alkyl thiophene)s induced by iodine doping as studied by an organized combination of X-ray diffraction, infrared/Raman spectroscopy and computer simulation techniques. *Polymer* **38**, 2867–2879 (1997).
77. Mai, C.-K. *et al.* Varying the ionic functionalities of conjugated polyelectrolytes leads to both p-and n-type carbon nanotube composites for flexible thermoelectrics. *Energy Environ. Sci.* **8**, 2341–2346 (2015).
78. Mai, C.-K. *et al.* Side-chain effects on the conductivity, morphology, and thermoelectric properties of self-doped narrow-band-gap conjugated polyelectrolytes. *J. Am. Chem. Soc.* **136**, 13478–13481 (2014).
79. Pingel, P. & Neher, D. Comprehensive picture of p-type doping of P3HT with the molecular acceptor F_4TCNQ. *Phys. Rev. B* **87**, 115209 (2013).
80. Xuan, Y. *et al.* Thermoelectric properties of conducting polymers: the case of poly (3-hexylthiophene). *Phys. Rev. B* **82**, 115454 (2010).
81. Wang, Z., Li, C., Scherr, E., MacDiarmid, A. & Epstein, A. Three dimensionality of 'metallic' states in conducting polymers: polyaniline. *Phys. Rev. Lett.* **66**, 1745 (1991).
82. Yoon, C. O. *et al.* Hopping transport in doped conducting polymers in the insulating regime near the metal–insulator boundary: polypyrrole, polyaniline and polyalkylthiophenes. *Synth. Met.* **75**, 229–239 (1995).
83. Paloheimo, J., Laakso, K., Isotalo, H. & Stubb, H. Conductivity, thermoelectric-power and field-effect mobility in self-assembled films of polyanilines and oligoanilines. *Synth. Met.* **68**, 249–257 (1995).
84. van de Ruit, K. *et al.* Quasi-one dimensional in-plane conductivity in filamentary films of PEDOT:PSS. *Adv. Funct. Mater.* **23**, 5778–5786 (2013).
85. Wang, S., Ha, M., Manno, M., Frisbie, C. D. & Leighton, C. Hopping transport and the Hall effect near the insulator–metal transition in electrochemically gated poly(3-hexylthiophene) transistors. *Nat. Commun.* **3**, 1210 (2012).
86. Epstein, A. *et al.* Inhomogeneous disorder and the modified Drude metallic state of conducting polymers. *Synth. Met.* **65**, 149–157 (1994).
87. Kim, Y. H. *et al.* Highly conductive PEDOT:PSS electrode with optimized solvent and thermal post-treatment for ITO-free organic solar cells. *Adv. Funct. Mater.* **21**, 1076–1081 (2011).
88. Luo, J. *et al.* Enhancement of the thermoelectric properties of PEDOT:PSS thin films by post-treatment. *J. Mater. Chem. A* **1**, 7576–7583 (2013).
89. DeLongchamp, D. M. *et al.* Influence of a water rinse on the structure and properties of poly(3,4-ethylene dioxythiophene): poly(styrene sulfonate) films. *Langmuir* **21**, 11480–11483 (2005).
90. Kim, G. H., Shao, L., Zhang, K. & Pipe, K. P. Engineered doping of organic semiconductors for enhanced thermoelectric efficiency. *Nat. Mater.* **12**, 719–723 (2013).
91. Scholes, D. T. *et al.* Overcoming film quality issues for conjugated polymers doped with F_4TCNQ by solution sequential processing: Hall effect, structural, and optical measurements. *J. Phys. Chem. Lett.* **6**, 4786–4793 (2015).
92. Lazzaroni, R., Lögdlund, M., Stafström, S., Salaneck, W. R. & Brēdas, J. L. The poly-3-hexylthiophene/NOPF6 system: a photoelectron spectroscopy study of electronic structural changes induced by the charge transfer in the solid state. *J. Chem. Phys.* **93**, 4433–4439 (1990).
93. Lögdlund, M., Lazzaroni, R., Stafström, S., Salaneck, W. R. & Brēdas, J. L. Direct observation of charge-induced π-electronic structural changes in a conjugated polymer. *Phys. Rev. Lett.* **63**, 1841–1844 (1989).
94. Yim, K. H. *et al.* Controlling electrical properties of conjugated polymers via a solution-based p-type doping. *Adv. Mater.* **20**, 3319–3324 (2008).
95. Bubnova, O. *et al.* Semi-metallic polymers. *Nat. Mater.* **13**, 190–194 (2014).
The first report of semi-metallic behaviour in an organic semiconductor resulting from the formation of bipolaron bands is presented in this work.
96. Aich, R. B., Blouin, N., Bouchard, A. & Leclerc, M. Electrical and thermoelectric properties of poly(2,7-carbazole) derivatives. *Chem. Mater.* **21**, 751–757 (2009).
97. Glaudell, A. M., Cochran, J. E., Patel, S. N. & Chabinyc, M. L. Impact of the doping method on conductivity and thermopower in semiconducting polythiophenes. *Adv. Energy Mater.* **5**, 1401072 (2015).
98. Zhang, F. J. *et al.* Modulated thermoelectric properties of organic semiconductors using field-effect transistors. *Adv. Funct. Mater.* **25**, 3004–3012 (2015).
99. Inabe, T. *et al.* Electronic structure of alkali metal doped C_{60} derived from thermoelectric-power measurements. *Phys. Rev. Lett.* **69**, 3797–3799 (1992).
100. Wang, Z. H. *et al.* Electronic transport properties of K_xC_{70} thin-films. *Phys. Rev. B* **48**, 10657–10660 (1993).
101. Sumino, M. *et al.* Thermoelectric properties of n-type C_{60} thin films and their application in organic thermovoltaic devices. *Appl. Phys. Lett.* **99,** 093308 (2011).
102. Sun, Y. M. *et al.* Organic thermoelectric materials and devices based on p- and n-type poly(metal 1,1,2,2-ethenetetrathiolate)s. *Adv. Mater.* **24**, 932–937 (2012).
The organometallic polymers presented in this study showcase organometallics as a promising class of high-performing p-type and n-type thermoelectric materials.
103. Kola, S. *et al.* Pyromellitic diimide–ethynylene-based homopolymer film as an n-channel organic field-effect transistor semiconductor. *ACS Macro Lett.* **2**, 664–669 (2013).
104. Fritzsche, H. A general expression for the thermoelectric power. *Solid State Commun.* **9**, 1813–1815 (1971).
105. Park, Y. W., Denenstein, A., Chiang, C. K., Heeger, A. J. & Macdiarmid, A. G. Semiconductor–metal transition in doped $(CH)_x$: thermoelectric power. *Solid State Commun.* **29**, 747–751 (1979).
106. Zhang, Q., Sun, Y. M., Xu, W. & Zhu, D. B. What to expect from conducting polymers on the playground of thermoelectricity: lessons learned from four high-mobility polymeric semiconductors. *Macromolecules* **47**, 609–615 (2014).
107. Reghu, M., Cao, Y., Moses, D. & Heeger, A. J. Counterion-induced processibility of polyaniline: transport at the metal–insulator boundary. *Phys. Rev. B* **47**, 1758–1764 (1993).
108. Yoon, C. O., Reghu, M., Moses, D. & Heeger, A. J. Transport near the metal–insulator-transition: polypyrrole doped with PF_6. *Phys. Rev. B* **49**, 10851–10863 (1994).
109. Nogami, Y. *et al.* On the metallic states in highly conducting iodine-doped polyacetylene. *Solid State Commun.* **76**, 583–586 (1990).
110. Kaiser, A. B. Electronic transport properties of conducting polymers and carbon nanotubes. *Rep. Prog. Phys.* **64**, 1 (2001).
111. Kaiser, A. B. Thermoelectric-power and conductivity of heterogeneous conducting polymers. *Phys. Rev. B* **40**, 2806–2813 (1989).
This paper reported an early analysis of how thermopower and electrical conductivity can vary due to percolation in organic materials.
112. Massonnet, N. *et al.* Improvement of the Seebeck coefficient of PEDOT:PSS by chemical reduction combined with a novel method for its transfer using free-standing thin films. *J. Mater. Chem. C* **2**, 1278–1283 (2014).
113. See, K. C. *et al.* Water-processable polymer–nanocrystal hybrids for thermoelectrics. *Nano Lett.* **10**, 4664–4667 (2010).
This study demonstrated that synergetic effects can be realized when rationally combining organic with inorganic thermoelectric materials, resulting in performance exceeding that of either of the individual components alone.
114. Massonnet, N., Carella, A., de Geyer, A., Faure-Vincent, J. & Simonato, J.-P. Metallic behaviour of acid doped highly conductive polymers. *Chem. Sci.* **6**, 412–417 (2015).
115. Pernstich, K. P., Rossner, B. & Batlogg, B. Field-effect-modulated Seebeck coefficient in organic semiconductors. *Nat. Mater.* **7**, 321–325 (2008).
116. Sun, J. *et al.* Simultaneous increase in Seebeck coefficient and conductivity in a doped poly(alkylthiophene) blend with defined density of states. *Macromolecules* **43**, 2897–2903 (2010).
117. Urban, J. J. Prospects for thermoelectricity in quantum dot hybrid arrays. *Nat. Nanotechnol.* **10**, 997–1001 (2015).
118. He, M. *et al.* Thermopower enhancement in conducting polymer nanocomposites via carrier energy scattering at the organic–inorganic semiconductor interface. *Energy Environ. Sci.* **5**, 8351–8358 (2012).
119. Zhou, C. *et al.* Nanowires as building blocks to fabricate flexible thermoelectric fabric: the case of copper telluride nanowires. *ACS Appl. Mater. Interface* **7**, 21015–21020 (2015).
120. Ju, Y. S., Kurabayashi, K. & Goodson, K. E. Thermal characterization of anisotropic thin dielectric films using harmonic Joule heating. *Thin Solid Films* **339**, 160–164 (1999).
121. Duda, J. C., Hopkins, P. E., Shen, Y. & Gupta, M. C. Exceptionally low thermal conductivities of films of the fullerene derivative PCBM. *Phys. Rev. Lett.* **110**, 015902 (2013).
122. Wang, X., Liman, C. D., Treat, N. D., Chabinyc, M. L. & Cahill, D. G. Ultralow thermal conductivity of fullerene derivatives. *Phys. Rev. B* **88**, 075310 (2013).
123. Wang, X., Ho, V., Segalman, R. A. & Cahill, D. G. Thermal conductivity of high-modulus polymer fibers. *Macromolecules* **46**, 4937–4943 (2013).
124. Liu, J. *et al.* Thermal conductivity and elastic constants of PEDOT:PSS with high electrical conductivity. *Macromolecules* **48**, 585–591 (2015).
125. Weathers, A. *et al.* Significant electronic thermal transport in the conducting polymer poly(3,4-ethylenedioxythiophene). *Adv. Mater.* **27**, 2101–2106 (2015).
126. Wei, Q., Mukaida, M., Kirihara, K. & Ishida, T. Experimental studies on the anisotropic thermoelectric properties of conducting polymer films. *ACS Macro Lett.* **3**, 948–952 (2014).
127. Arias, A. C., MacKenzie, J. D., McCulloch, I., Rivnay, J. & Salleo, A. Materials and applications for large area electronics: solution-based approaches. *Chem. Rev.* **110**, 3–24 (2010).
128. Rogers, J. A., Someya, T. & Huang, Y. Materials and mechanics for stretchable electronics. *Science* **327**, 1603–1607 (2010).
129. Schwartz, G. *et al.* Flexible polymer transistors with high pressure sensitivity for application in electronic skin and health monitoring. *Nat. Commun.* **4**, 1859 (2013).
130. Leonov, V. in *Wearable Monitoring Systems* (eds Bonfiglio, A. & De Rossi, D.) 27–49 (Springer, 2011).
131. Sun, T., Peavey, J. L., David Shelby, M., Ferguson, S. & O'Connor, B. T. Heat shrink formation of a corrugated thin film thermoelectric generator. *Energy Convers. Manage.* **103**, 674–680 (2015).
132. Goldsmid, H. (ed.) *Thermoelectric Refrigeration* (Springer, 2013).

133. Goupil, C., Seifert, W., Zabrocki, K., Müller, E. & Snyder, G. J. Thermodynamics of thermoelectric phenomena and applications. *Entropy* **13**, 1481–1517 (2011).
134. Bahk, J.-H., Fang, H., Yazawa, K. & Shakouri, A. Flexible thermoelectric materials and device optimization for wearable energy harvesting. *J. Mater. Chem. C* **3**, 10362–10374 (2015).
135. Owoyele, O., Ferguson, S. & O'Connor, B. T. Performance analysis of a thermoelectric cooler with a corrugated architecture. *Appl. Energy* **147**, 184–191 (2015).
136. Fujifilm. *Sustainability Report 2013*, 18–19 (Fujifilm, 2013).
137. Kim, S. J., We, J. H. & Cho, B. J. A wearable thermoelectric generator fabricated on a glass fabric. *Energy Environ. Sci.* **7**, 1959–1965 (2014).
138. Madan, D., Wang, Z., Wright, P. K. & Evans, J. W. Printed flexible thermoelectric generators for use on low levels of waste heat. *Appl. Energy* **156**, 587–592 (2015).
139. Du, Y. *et al.* Thermoelectric fabrics: toward power generating clothing. *Sci. Rep.* **5**, 6411 (2015).
140. Nonoguchi, Y. *et al.* Systematic conversion of single walled carbon nanotubes into n-type thermoelectric materials by molecular dopants. *Sci. Rep.* **3**, 3344 (2013).
141. Yu, C. H., Murali, A., Choi, K. W. & Ryu, Y. Air-stable fabric thermoelectric modules made of n- and p-type carbon nanotubes. *Energy Environ. Sci.* **5**, 9481–9486 (2012).
142. Søndergaard, R. R., Hösel, M., Espinosa, N., Jørgensen, M. & Krebs, F. C. Practical evaluation of organic polymer thermoelectrics by large-area R2R processing on flexible substrates. *Energy Sci. Eng.* **1**, 81–88 (2013).
143. Tomlinson, E. P., Hay, M. E. & Boudouris, B. W. Radical polymers and their application to organic electronic devices. *Macromolecules* **47**, 6145–6158 (2014).
144. Tomlinson, E. P., Willmore, M. J., Zhu, X., Hilsmier, S. W. A. & Boudouris, B. W. Tuning the thermoelectric properties of a conducting polymer through blending with open-shell molecular dopants. *ACS Appl. Mater. Interface* **7**, 18195–18200 (2015).
145. Stavrinidou, E. *et al.* Direct measurement of ion mobility in a conducting polymer. *Adv. Mater.* **25**, 4488–4493 (2013).
146. Wang, H., Ail, U., Gabrielsson, R., Berggren, M. & Crispin, X. Ionic Seebeck effect in conducting polymers. *Adv. Energy Mater.* **5**, 1500044 (2015).
147. Chang, W. B. *et al.* Harvesting waste heat in unipolar ion conducting polymers. *ACS Macro Lett.* **5**, 94–98 (2016).
148. Chang, W. B. *et al.* Electrochemical effects in thermoelectric polymers. *ACS Macro Lett.* **5**, 455–459 (2016).
149. Bell, L. E. Cooling, heating, generating power, and recovering waste heat with thermoelectric systems. *Science* **321**, 1457–1461 (2008).
150. Onda, K., Masuda, T., Nagata, S. & Nozaki, K. Cycle analyses of thermoelectric power generation and heat pumps using the β″-alumina electrolyte. *J. Power Sources* **55**, 231–236 (1995).
151. Bian, Z. & Shakouri, A. Beating the maximum cooling limit with graded thermoelectric materials. *Appl. Phys. Lett.* **89**, 212101 (2006).
152. Snyder, G. J., Fleurial, J.-P., Caillat, T., Yang, R. & Chen, G. Supercooling of peltier cooler using a current pulse. *J. Appl. Phys.* **92**, 1564–1569 (2002).
153. Zhang, F., Zang, Y., Huang, D., Di, C.-a. & Zhu, D. Flexible and self-powered temperature–pressure dual-parameter sensors using microstructure-frame-supported organic thermoelectric materials. *Nat. Commun.* **6,** 8356 (2015).
154. Yazawa, K. & Shakouri, A. Scalable cost/performance analysis for thermoelectric waste heat recovery systems. *J. Electron. Mater.* **41**, 1845–1850 (2012).
155. Yee, S. K., LeBlanc, S., Goodson, K. E. & Dames, C. $ per W metrics for thermoelectric power generation: beyond *ZT*. *Energy Environ. Sci.* **6**, 2561–2571 (2013).
Important conceptual introduction of alternative metrics to ZT that may better capture the merits of using scalable, flexible thermoelectric devices.
156. Darian-Smith, I. in *Comprehensive Physiology* (Wiley, 2011).
157. Cho, C. *et al.* Completely organic multilayer thin film with thermoelectric power factor rivaling inorganic tellurides. *Adv. Mater.* **27**, 2996–3001 (2015).

Acknowledgements
The authors acknowledge support from the AFOSR-MURI on Controlling Thermal and Electrical Transport in Organic and Hybrid Materials, AFOSR MURI FA9550-12-1-0002, as well as the Molecular Foundry, a LBNL user facility supported by the Office of Science, BES, US DOE, under Contract DE-AC02-05CH11231.

Competing interests statement
The authors declare no competing interests.